Dark Photon Oscillations in Our Inhomogeneous Universe

Andrea Caputo[1,*] Hongwan Liu[2,3,†] Siddharth Mishra-Sharma[2,‡] and Joshua T. Ruderman[2,§]

^{1}*Instituto de Física Corpuscular, CSIC-Universitat de Valencia, Apartado de Correos 22085, E-46071, Valencia, Spain*
^{2}*Center for Cosmology and Particle Physics, Department of Physics, New York University, New York, New York 10003, USA*
^{3}*Department of Physics, Princeton University, Princeton, New Jersey 08544, USA*

A dark photon kinetically mixing with the ordinary photon represents one of the simplest viable extensions to the standard model, and would induce oscillations with observable imprints on cosmology. Oscillations are resonantly enhanced if the dark photon mass equals the ordinary photon plasma mass, which tracks the free electron number density. Previous studies have assumed a homogeneous Universe; in this Letter, we introduce for the first time an analytic formalism for treating resonant oscillations in the presence of inhomogeneities of the photon plasma mass. We apply our formalism to determine constraints from cosmic microwave background photons oscillating into dark photons, and from heating of the primordial plasma due to dark photon dark matter converting into low-energy photons. Including the effect of inhomogeneities demonstrates that prior homogeneous constraints are not conservative, and simultaneously extends current experimental limits into a vast new parameter space.

Introduction.—A minimal extension of the standard model (SM) is a dark photon, A', kinetically mixing [1] with the ordinary photon, γ. Kinetic mixing is one of a few portals allowing new physics to couple to the standard model through a dimensionless interaction that can be manifest at low energies. Further motivations for dark photons is that they may constitute dark matter [2–12] and are ubiquitous in theories beyond the SM [13–19]. Very light dark photons decouple from experiments as a positive power of $m_{A'}/E_{\rm exp}$, where $m_{A'}$ is the mass of the dark photon and $E_{\rm exp}$ is the experimental energy scale. Because of this decoupling behavior, light dark photons with sizable interactions are consistent with current experimental constraints.

Kinetic mixing induces oscillations of photons into dark photons, $\gamma \rightarrow A'$, as well as the reverse process, $A' \rightarrow \gamma$. In the early Universe, given a redshift z and position $\vec{x}$, the photon has a plasma mass, $m_\gamma(z, \vec{x})$, that tracks the free electron number density, $n_e(z, \vec{x})$. The oscillation probability is resonantly enhanced if the plasma mass equals the mass of the dark photon, $m_\gamma(z, \vec{x}) \approx m_{A'}$. We consider massive dark photons, with a mass in the interval $10^{-14} \lesssim m_{A'} \lesssim 10^{-9}$ eV, the homogeneous (spatially averaged) value of the plasma mass, $\bar{m}_\gamma(z)$, crosses the dark photon mass after recombination. In this regime there are powerful constraints [20,21] from $\gamma \rightarrow A'$ oscillations distorting the shape of the cosmic microwave background (CMB) spectrum measured by FIRAS [22]. Dark matter composed of dark photons is also constrained by heating of the primordial plasma from resonant $A' \rightarrow \gamma$ oscillations [23], producing low-energy photons that are efficiently absorbed by baryons. Additional constraints on dark photon dark matter are considered by Refs. [4,24–26].

Previous studies of cosmological dark photon oscillations have assumed a homogeneous plasma mass, i.e., $m_\gamma(z, \vec{x}) \approx \bar{m}_\gamma(z)$. However, the plasma mass has perturbations that track inhomogeneities in the electron number density, which are a predicted consequence of the growth of structure in the early Universe. Consider a photon that propagates along a worldline through the primordial plasma. In the homogeneous limit, this photon may experience a level crossing at a specific redshift, $z_{\rm res}$, when $\bar{m}_\gamma(z_{\rm res}) \approx m_{A'}$. In reality, a photon's path traverses regions with overdensities and underdensities, and may pass through many different level crossings at redshifts that differ from $z_{\rm res}$. Figure 1 shows a simulation of this process for a dark photon mass with $z_{\rm res} \approx 100$; perturbations in the plasma mass induce resonant conversions over a wide range of redshifts, $90 \lesssim z \lesssim 110$. The effect of inhomogeneities is especially dramatic for dark photons with masses $m_{A'} \lesssim 10^{-14}$ eV, which experience no level crossings in the homogeneous limit, but in reality can experience level crossings in regions with lower-than-average electron number density.

This Letter is part of a pair of companion papers in which we initiate the study of resonant oscillations between photons and dark photons in the presence of inhomogeneities in the photon plasma mass. We introduce an analytic formalism for calculating the probability that photons or dark photons oscillate as they travel through the inhomogeneous plasma. As applications of our formalism, we revisit bounds from the CMB spectrum on photons oscillating to dark photons, $\gamma \rightarrow A'$, and bounds from energy injection due to dark photon dark matter oscillating into ordinary photons, $A' \rightarrow \gamma$. We find that these bounds
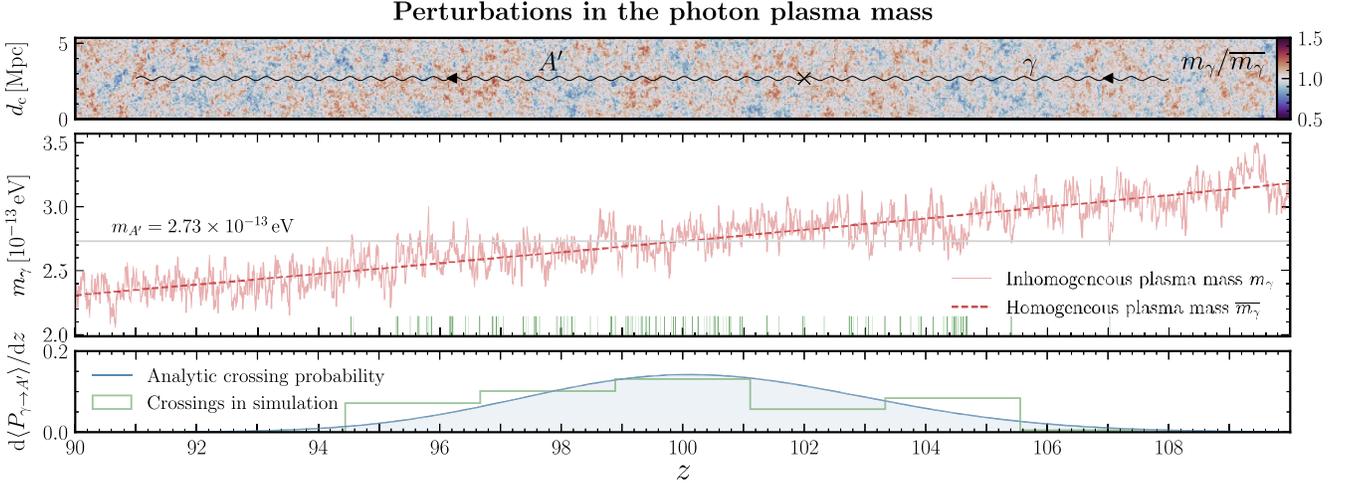
FIG. 1. (Top) A simulated realization of the plasma mass in a box of comoving thickness 5 Mpc, centered around $z = 100$. An example photon path with conversion to a dark photon at the redshift marked "$\times$" is shown. (Middle) A line-of-sight section through the perturbed plasma mass (solid red line), as might be encountered by a traversing CMB photon, compared to the homogeneous plasma mass (dashed red line). For a dark photon mass of $m_{A'} = 2.73 \times 10^{-13}$ eV, the corresponding homogeneous transition occurs at $z \simeq 100$ where the plasma mass reaches $m_{A'}$ (gray line). Multiple level crossings are possible after accounting for perturbations—individual crossings in this realization are shown as the vertical green lines. (Bottom) The corresponding analytical differential conversion probability (blue line) and a histogram of the crossing density corresponding to the specific realization shown (green) [27].

require significant revision: compared to the homogeneous limit, perturbations both induce new resonances in underdensities and overdensities, extending these bounds into a vast new parameter space, and can also wash out resonances, making the sensitivity derived in the homogeneous approximation an overestimate for certain dark photon masses. The homogeneous limit is therefore not a conservative approximation of our inhomogeneous Universe.

Dark photons with masses $10^{-15} \lesssim m_{A'} \lesssim 10^{-9}$ eV are the target of several planned experiments using resonant detectors. DM Radio targets dark photon dark matter [28,29], while Dark SRF [30,31] aims to produce and detect dark photons without assuming a cosmic abundance [32].

In our companion paper [33] we examine the physics of oscillations in detail, giving a derivation of our formalism together with a complete description of the cosmological inputs that are required to derive the limits shown here. We also validate our analytical results with simulations of $\gamma \to A'$ oscillations.

The remainder of this Letter is organized as follows. We begin by reviewing $\gamma \leftrightarrow A'$ oscillations. We then introduce our analytic formalism for treating these oscillations in the presence of perturbations of the photon plasma mass. Next, we apply our formalism to determine the constraints on $\gamma \to A'$ oscillations from FIRAS data. We then show how inhomogeneities extend constraints on energy injection from dark photon dark matter to new dark photon masses. Our conclusions highlight additional possible applications and extensions of our formalism. Throughout this work, we use units with $\hbar = c = k_B = 1$, and the Planck 2018 cosmology [34].

Resonant photon-dark photon oscillations.—We consider the following photon-dark photon Lagrangian:

$$\mathcal{L}_{\gamma A'} = -\frac{1}{4}F_{\mu\nu}^2 - \frac{1}{4}(F'_{\mu\nu})^2 - \frac{\epsilon}{2}F^{\mu\nu}F'_{\mu\nu} + \frac{1}{2}m_{A'}^2(A'_\mu)^2, \quad (1)$$

where ϵ is a dimensionless measure of kinetic mixing with typical "natural" values in the range 10^{-13}–10^{-2} eV [13,17–19,35]. A' is the dark photon field, with F and F' representing the field strength tensor for the photon and dark photon, respectively.

The propagation of CMB photons in the primordial plasma leads to in-medium effects that are described by a mass term, m_γ, in the photon dispersion relation. There are positive and negative contributions to m_γ^2 from scattering off free electrons and neutral atoms, respectively [20,21]:

$$m_\gamma^2(z, \vec{x}) \simeq 1.4 \times 10^{-21} \text{ eV}^2 \left(\frac{n_e(z, \vec{x})}{\text{cm}^{-3}}\right)$$
$$-8.4 \times 10^{-24} \text{ eV}^2 \left(\frac{\omega(z)}{\text{eV}}\right)^2 \left(\frac{n_{\text{HI}}(z, \vec{x})}{\text{cm}^{-3}}\right), \quad (2)$$

where $\omega(z)$ is the photon energy, and $n_e(z, \vec{x})$ and $n_{\text{HI}}(z, \vec{x})$ represent the local free electron and neutral hydrogen densities. We model the evolution of cosmological quantities using CLASS [36] interfaced with HyRec [37]. For $\epsilon \ll 1$, $\gamma \to A'$ conversion is a resonant process that is efficient only when the dark photon mass is equal to the plasma mass; in this limit, we can apply the Landau-Zener approximation for nonadiabatic transitions [20,33,38,39],
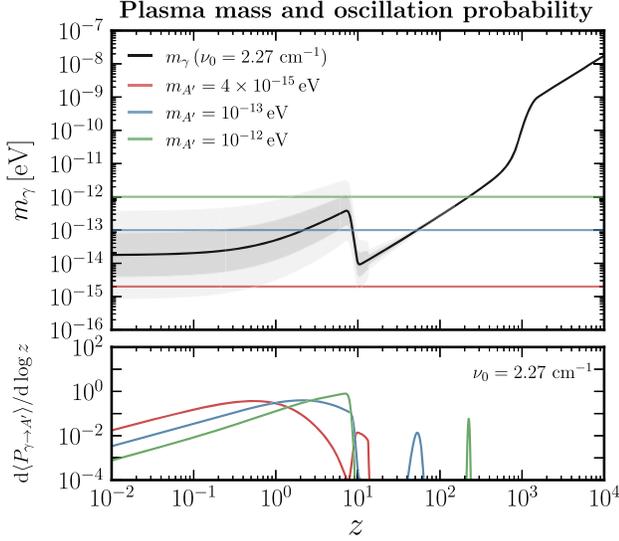
FIG. 2. (Top) The photon plasma mass as a function of redshift corresponding to the lowest-frequency FIRAS band ($\nu_0 = 2.27$ cm^{-1}), which dominates the total conversion probability. The middle 68% and 95% containment of plasma mass fluctuations in the log-normal prescription is shown in dark and light gray, respectively. Horizontal lines correspond to the fiducial mass points $m_{A'} = 4 \times 10^{-15}$ (red), 10^{-13} (blue), and 10^{-12} eV (green), respectively. (Bottom) The differential resonant transition probability for this frequency as a function of redshift for the fiducial masses, normalized to unity total probability, showing efficient conversion probability over a wide range of redshifts [58].

$$P_{\gamma \to A'} \simeq \sum_i \frac{\pi m_{A'}^2 \epsilon^2}{\omega(t_i)} \left| \frac{d \ln m_\gamma^2(t)}{dt} \right|_{t=t_i}^{-1}, \quad (3)$$

where i indexes times t_i when $m_\gamma^2(t_i) = m_{A'}^2$ and therefore the resonance condition is met. Equation (3) describes the probability that a photon will convert along its path, which depends on $m_\gamma(t)$ along this path. Equation (3) assumes $P_{\gamma \to A'} \ll 1$, which applies throughout this work. Similar results have also been derived in the context of neutrino oscillations in supernovae [40–42].

The effect of inhomogeneities.—Inhomogeneities in the photon plasma mass substantially affect the conversion probability of photons into dark photons and vice versa, allowing for efficient oscillations over a range of cosmic times rather than at a single epoch.

In the presence of plasma mass inhomogeneities, we need to take the average of Eq. (3) over different photon paths to account for transitions in locally overdense and underdense regions. This problem reduces to integrating over m_γ^2 at each point in time, weighted by the probability density function of finding a region with plasma mass m_γ^2. Our formalism draws from Rice's formula for the average number of level crossings of a random field [43,44]. In our companion paper [33], we derive the following differential conversion probability:

$$\frac{d\langle P_{\gamma \to A'} \rangle}{dz} = \frac{\pi m_{A'}^2 \epsilon^2}{\omega(t)} \left| \frac{dt}{dz} \right|$$
$$\times \int dm_\gamma^2 f(m_\gamma^2; t) \delta_D(m_\gamma^2 - m_{A'}^2) m_\gamma^2, \quad (4)$$

where $f(m_\gamma^2; t)$ is the probability density function (PDF) of m_γ^2 at time t, and δ_D is the Dirac delta distribution. Neglecting perturbations in the free electron fraction x_e (see Ref. [33] for a discussion on why this assumption is valid here), Eq. (2) shows that $m_\gamma^2(z, \vec{x}) \propto n_b(z, \vec{x})$, where n_b is the baryon number density; this implies that

$$f(m_\gamma^2; t) = \mathcal{P}(\delta_b; t) / \overline{m_\gamma^2}, \quad (5)$$

where $\mathcal{P}(\delta_b; t)$ is the one-point PDF of baryon density fluctuations $\delta_b \equiv (n_b - \bar{n}_b)/\bar{n}_b$ and $\overline{m_\gamma^2}$ the average squared plasma mass. Equation (5) therefore ties the physics of $\gamma \leftrightarrow A'$ directly to a cosmological observable. The proportionality $m_\gamma^2 \propto n_b$ together with the definition of δ_b implies that that $1 + \delta_b = m_\gamma^2 / \overline{m_\gamma^2}$.

Equation (4) is one of our main results, and we consider a few different possibilities for the one-point PDF $\mathcal{P}(\delta_b; t)$ in order to estimate the theoretical uncertainty associated with the nonlinear distribution of matter at low redshifts $z \lesssim 6$. First, we consider a log-normal distribution, which has long been used as a simple model for the distribution of the low-redshift matter density [45–48]. To inform the spectrum of fluctuations for this distribution, we use the baryonic power spectra $P_{bb}(k)$ derived from hydrodynamic simulations [49–52] and extracted in Refs. [53,54]. Second, we adopt an analytical prescription [55], which extends the spherical collapse model [56,57] to perform a first-principles computation of the nonlinear matter PDF.

In the literature, $\mathcal{P}(\delta_b; t)$ is typically defined as a function of a smoothing scale R over which densities are averaged in order to match observations and simulation results; furthermore, the width of the distribution can exhibit a log-divergence in R if $P_{bb}(k) \propto k^{-3}$ at large k. In our work, we assume that baryonic structures are suppressed on scales smaller than the baryonic Jeans scale $R_J \sim 10$ kpc. In practice, the log-normal PDF is computed with a $P_{bb}(k)$ which has a cutoff at $k_J \sim 1/R_J$ derived from CLASS, while our analytic PDF is obtained with a smoothing scale $R = R_J$. A complete description of our PDFs and the Jeans scale is given in Ref. [33].

The differential transition probability (normalized to unity) for a few benchmark dark photon mass points $m_{A'} = 2 \times 10^{-15}, 10^{-13}$, and 10^{-12} eV is shown in the bottom panel of Fig. 2. For $m_{A'} = 10^{-12}$ eV there is a narrow resonance corresponding to a transition in the limit of a homogeneous plasma at $z \sim 200$. An additional broad resonance at $z \sim 6$ is also present, corresponding to conversions in overdensities in the plasma mass post-reionization. Note that Eq. (3) implies that later resonances typically contribute more to the total conversion
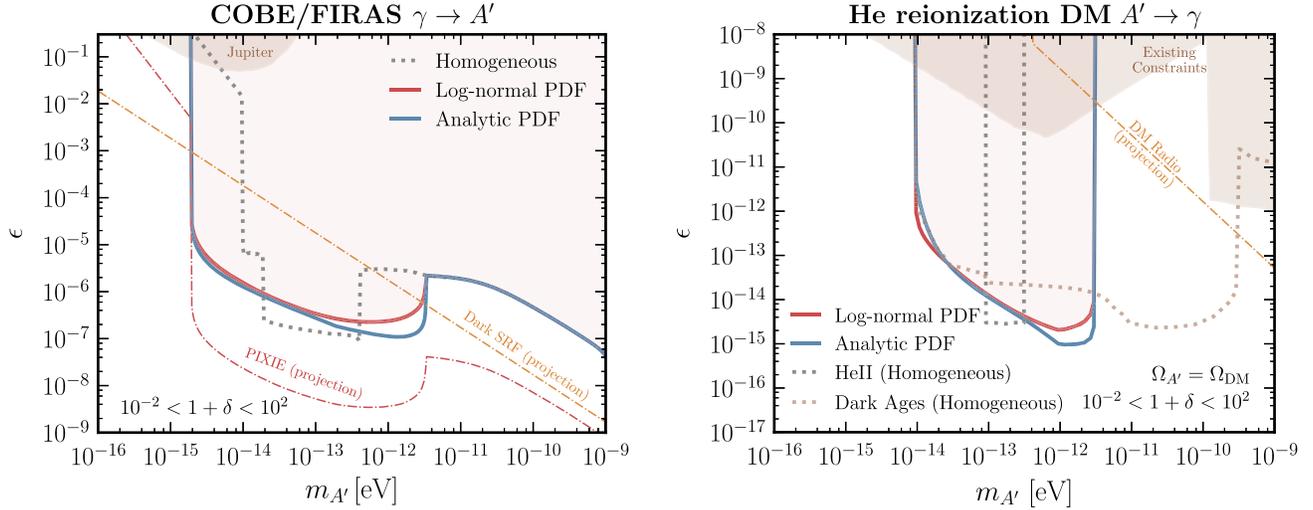
FIG. 3.   (Left) The 95% confidence level constraints on the kinetic mixing parameter ϵ as a function of dark photon mass $m_{A'}$, assuming log-normal (red line) or analytic (blue line) PDFs; the shaded region is ruled out by the more conservative of the two PDF choices. We also show the reach of the proposed PIXIE satellite [79] (dot-dashed red line) assuming a log-normal PDF. For comparison we show the previous limit assuming a homogeneous plasma (dotted gray line), a constraint from the magnetic field of Jupiter [80,84] (shaded brown), and the projected reach of the Dark SRF experiment [30,31] (dot-dashed orange line), which would be complementary to our cosmological constraints. (Right) Constraints on dark photon dark matter from anomalous heating of the IGM during the epoch of HeII reionization, for the same PDFs. Prior constraints (shaded brown) come from nonresonant heating of the IGM [23] and heating of the gas in the dwarf galaxy Leo T [26]. We also show the projected reach of DM Radio Stage 3 [28,29,85] (dot-dashed orange line). Limits from changes to the dark matter density and from IGM heating during the dark ages assuming a homogeneous plasma mass have been derived in Ref. [23] (dotted orange line) [86,87].

probability. For $m_{A'} = 2 \times 10^{-15}$ eV, no resonance exists in the homogeneous limit; remarkably, however, fluctuations in the plasma mass result in resonant transitions over a broad range of redshifts at $z \lesssim 20$ due to underdensities in the plasma mass. This opens up the possibility of probing dark photon masses $m_{A'} \lesssim 10^{-14}$ eV through previously neglected cosmological conversions.

Dark photon oscillations in the CMB spectrum.—We first apply our formalism to analyze the intensity of the CMB as measured by the FIRAS instrument aboard COBE [22] for evidence of deviations from a blackbody spectrum due to $\gamma \to A'$ oscillations. Notably in this case the dark photon does not need to be the dark matter. The spectrum of the FIRAS data is fit by the nearly perfectly Planckian spectrum B_ω with temperature $T_{\mathrm{CMB}} = 2.725$ K [59]. For a given dark photon model specified by its mass $m_{A'}$ and mixing parameter ϵ, the spectral distortion to the CMB spectrum will be given by $I_{\omega_0}(m_{A'}, \epsilon) = B_{\omega_0}(1 - \langle P_{\gamma \to A'} \rangle)$, where $\langle P_{\gamma \to A'} \rangle$ is the conversion probability for the given model corresponding to the present-day frequency ω_0, obtained by integrating Eq. (4). Details of the data analysis are presented in the Supplemental Material [60].

Erring on the conservative side, we do not consider fluctuations outside of the range $10^{-2} < 1 + \delta_b < 10^2$, and as such our results do not rely on conversions in the tails of the PDF where uncertainties are large. Additionally, for all cases considered here conversions in the redshift range $6 < z < 20$ have been excised, providing a conservative

result while being agnostic to the uncertainties arising from the complex physics of reionization in this epoch. We explore the effects of these choices in the Supplemental Material [60].

We observe no significant evidence for a signal. In the left panel of Fig. 3 we show our fiducial constraints at the 95% confidence level on the dark photon mixing parameter ϵ for a range of dark photon masses $m_{A'}$. We show constraints using both the log-normal and analytic description of the PDF. We also show the projected limits for a future measurement of the CMB spectrum such as the proposed PIXIE satellite [79] using the putative specifications from Ref. [21]. The traditional constraint assuming a homogeneous plasma mass as a function of redshift is also shown for comparison, together with constraints projected by the resonant cavity-based Dark SRF experiment [30,31] and existing constraints from an analysis of the magnetic field of Jupiter [80]. There are bounds from black hole superradiance for values of $m_{A'}$ that overlap our bounds assuming $\epsilon = 0$ [81–83], but it is unknown if these apply when $\epsilon > 0$ implying interactions of A' with plasma around the black hole.

Dark photon dark matter.—So far, we have studied the resonant conversion of CMB photons into relativistic ($v \simeq c$) dark photons. A cold, nonrelativistic ($v \ll c$) population of dark photons can also be produced non-thermally in the early Universe, and is a good candidate for dark matter [2,4,8,10,12]. Additional constraints apply in

this case; in particular, Ref. [23] proposed using measurements of the temperature of the intergalactic medium (IGM) around the epoch of HeII reionization ($2 \lesssim z \lesssim 6$) [61,88–92] to constrain the dark photon dark matter scenario. These measurements show that during HeII reionization, the total heat input per baryon is on the order of 1 eV. $A' \to \gamma$ conversion for light A''s produce soft photons that are absorbed efficiently through free-free absorption, leading to an anomalous heating of the IGM. The derived bound in the homogeneous limit extends over a limited mass range, precisely where the dark photon mass matches the homogeneous plasma mass in the narrow redshift range $2 \lesssim z \lesssim 6$. Our formalism accounting for inhomogeneities extends this treatment to a wider range of dark photon masses.

The total energy injected per unit baryon $\langle E_{A' \to \gamma} \rangle$ from the dark matter can be computed as

$$\frac{d\langle E_{A' \to \gamma} \rangle}{dz} = \pi m_{A'} \epsilon^2 \frac{\bar{\rho}_{A'}}{\bar{n}_b} \left| \frac{dt}{dz} \right|$$
$$\times \int dm_\gamma^2 \frac{m_\gamma^2}{\overline{m_\gamma^2(t)}} f(m_\gamma^2; t) \delta_D(m_\gamma^2 - m_{A'}^2) m_\gamma^2, \quad (6)$$

where $\bar{\rho}_{A'}/\bar{n}_b$ is the ratio of the homogeneous dark matter energy density to baryon number density, which is a time-independent quantity (we assume that the deposited heat from A' conversions is shared equally among all baryons: for further discussion of this assumption, we refer the reader to the Supplemental Material [60]). The total energy injected is then obtained by performing an integral over $2 < z < 6$. Considering the same PDFs discussed in the previous section and imposing $\langle E_{A' \to \gamma} \rangle < 1$ eV, we derive the constraints shown in the right panel of Fig. 3, with the homogeneous limit shown for comparison. Also shown is the parameter space covered by existing constraints [23,26], as well as the projected constraints from DM Radio Stage 3 [28,29,85]. Finally, our limits can be rescaled as a function of the maximum $\langle E_{A' \to \gamma} \rangle$ allowed and $\rho_{A'}$ by noting that $\langle E_{A' \to \gamma} \rangle \propto \epsilon^2 \rho_{A'}$.

Conclusions.—We have introduced a framework for treating oscillations between dark photons and ordinary photons as they traverse the inhomogeneous plasma of our Universe. Our main results are Eqs. (4) and (6). A complete discussion and derivation of these results appear in our companion paper [33]. We have applied this framework to determine constraints from CMB photons oscillating into dark photons (Fig. 3, left panel) and from energy injection from dark photon dark matter (Fig. 3, right panel). Prior studies have assumed the homogeneous limit and require significant revision because inhomogeneities both extend the mass reach, and either strengthen or weaken the sensitivity for masses constrained in the homogeneous limit.

We anticipate broader applications of our framework. Perturbations in the photon plasma mass will modify resonant oscillations of photons into axionlike particles, which can occur in the presence of primordial magnetic fields [93] or dark magnetic fields [94]. Here we have considered oscillations of dark photon dark matter, but dark photons (or axionlike particles) can also resonantly inject photons that impact 21 cm observations [94–96]. We have here considered global (sky-averaged) effects, but photon-to-dark photon oscillations in an inhomogeneous background will imprint anisotropies in the CMB that may be testable by Planck [34] and/or next-generation probes of CMB anisotropies [97,98].

Additional details of the data analysis performed and a discussion of systematic effects is presented in the Supplemental Material [60]. A much more in-depth discussion of our formalism, the choice of one-point PDFs, the construction of the baryon power spectrum, and a verification of our formalism with simulations are all discussed in our companion paper [33]. The code used to obtain the results in this Letter, our companion paper [33], as well as digitized constraints are available at Ref. [99].

The supporting data for this Letter are openly available from GitHub [27,58,86,87,99].

* andrea.caputo@uv.es
† hongwanl@princeton.edu
‡ sm8383@nyu.edu
§ ruderman@nyu.edu

[1] B. Holdom, Phys. Lett. B 166B, 196 (1986).
[2] J. Redondo and M. Postma, J. Cosmol. Astropart. Phys. 02 (2009) 005.
[3] A. E. Nelson and J. Scholtz, Phys. Rev. D 84, 103501 (2011).
[4] P. Arias, D. Cadamuro, M. Goodsell, J. Jaeckel, J. Redondo, and A. Ringwald, J. Cosmol. Astropart. Phys. 06 (2012) 013.
[5] A. Fradette, M. Pospelov, J. Pradler, and A. Ritz, Phys. Rev. D 90, 035022 (2014).
[6] H. An, M. Pospelov, J. Pradler, and A. Ritz, Phys. Lett. B 747, 331 (2015).
[7] P. W. Graham, J. Mardon, and S. Rajendran, Phys. Rev. D 93, 103520 (2016).
[8] P. Agrawal, N. Kitajima, M. Reece, T. Sekiguchi, and F. Takahashi, Phys. Lett. B 801, 135136 (2020).
[9] J. A. Dror, K. Harigaya, and V. Narayan, Phys. Rev. D 99, 035036 (2019).
[10] R. T. Co, A. Pierce, Z. Zhang, and Y. Zhao, Phys. Rev. D 99, 075002 (2019).
[11] M. Bastero-Gil, J. Santiago, L. Ubaldi, and R. Vega-Morales, J. Cosmol. Astropart. Phys. 04 (2019) 015.
[12] A. J. Long and L.-T. Wang, Phys. Rev. D 99, 063529 (2019).
[13] K. R. Dienes, C. F. Kolda, and J. March-Russell, Nucl. Phys. B492, 104 (1997).
[14] M. Goodsell, J. Jaeckel, J. Redondo, and A. Ringwald, J. High Energy Phys. 11 (2009) 027.
[15] M. Goodsell and A. Ringwald, Fortschr. Phys. 58, 716 (2010).
[16] M. Goodsell, in 5th Patras Workshop on Axions, WIMPs and WISPs, edited by J. Jaeckel, A. Lindner, and J. Redondo (Verlag Deutsches Elektronen-Synchrotron, 2009), pp. 165–168, http://www-library.desy.de/preparch/desy/proc/proc09-05.pdf.
[17] S. A. Abel and B. W. Schofield, Nucl. Phys. B685, 150 (2004).
[18] S. A. Abel, J. Jaeckel, V. V. Khoze, and A. Ringwald, Phys. Lett. B 666, 66 (2008).
[19] S. A. Abel, M. D. Goodsell, J. Jaeckel, V. V. Khoze, and A. Ringwald, J. High Energy Phys. 07 (2008) 124.
[20] A. Mirizzi, J. Redondo, and G. Sigl, J. Cosmol. Astropart. Phys. 03 (2009) 026.
[21] K. E. Kunze and M. Á. Vázquez-Mozo, J. Cosmol. Astropart. Phys. 12 (2015) 028.
[22] D. J. Fixsen, E. S. Cheng, J. M. Gales, J. C. Mather, R. A. Shafer, and E. L. Wright, Astrophys. J. 473, 576 (1996).
[23] S. D. McDermott and S. J. Witte, Phys. Rev. D 101, 063030 (2020).
[24] S. Dubovsky and G. Hernández-Chifflet, J. Cosmol. Astropart. Phys. 12 (2015) 054.
[25] E. D. Kovetz, I. Cholis, and D. E. Kaplan, Phys. Rev. D 99, 123511 (2019).
[26] D. Wadekar and G. R. Farrar, arXiv:1903.12190.
[27] A. Caputo, H. Liu, S. Mishra-Sharma, and J. T. Ruderman (2020), https://github.com/smsharma/dark-photons-perturbations/blob/apr-2020/notebooks/03_simulations.ipynb.
[28] S. Chaudhuri, P. W. Graham, K. Irwin, J. Mardon, S. Rajendran, and Y. Zhao, Phys. Rev. D 92, 075012 (2015).
[29] M. Silva-Feaver et al., IEEE Trans. Appl. Supercond. 27, 1400204 (2017).
[30] R. Harnik, Dark SRF—Theory (2019), 2019 PAC Meeting.
[31] A. Grassellino, Dark SRF—Experiment (2019), 2019 PAC Meeting.
[32] P. W. Graham, J. Mardon, S. Rajendran, and Y. Zhao, Phys. Rev. D 90, 075017 (2014).
[33] A. Caputo, H. Liu, S. Mishra-Sharma, and J. T. Ruderman, companion paper, Phys. Rev. D 102, 103533 (2020).
[34] N. Aghanim et al. (Planck Collaboration), Astron. Astrophys. 641, A6 (2020).
[35] T. Gherghetta, J. Kersten, K. Olive, and M. Pospelov Phys. Rev. D 100, 095001 (2019).
[36] D. Blas, J. Lesgourgues, and T. Tram, J. Cosmol. Astropart. Phys. 07 (2011) 034.
[37] Y. Ali-Haimoud and C. M. Hirata, Phys. Rev. D 83, 043513 (2011).
[38] T.-K. Kuo and J. T. Pantaleone, Rev. Mod. Phys. 61, 937 (1989).
[39] S. J. Parke, Phys. Rev. Lett. 57, 1275 (1986).
[40] B. Dasgupta and A. Dighe, Phys. Rev. D 75, 093002 (2007).
[41] A. Friedland and A. Gruzinov, arXiv:astro-ph/0607244.
[42] G. L. Fogli, E. Lisi, A. Mirizzi, and D. Montanino, J. Cosmol. Astropart. Phys. 06 (2006) 012.
[43] S. O. Rice, Bell Syst. Tech. J. 23, 282 (1944).
[44] G. Lindgren, Stationary Stochastic Processes: Theory and Applications (Chapman & Hall/CRC Texts in Statistical Science, Taylor & Francis, Oxford, 2012).
[45] E. Hubble, Astrophys. J. 79, 8 (1934).
[46] P. Coles and B. Jones, Mon. Not. R. Astron. Soc. 248, 1 (1991).
[47] I. Kayo, A. Taruya, and Y. Suto, Astrophys. J. 561, 22 (2001).
[48] V. Wild et al. (2dFGRS Collaboration), Mon. Not. R. Astron. Soc. 356, 247 (2005).
[49] D. Nelson et al., arXiv:1812.05609.
[50] S. McAlpine et al., Astron. Comput. 15, 72 (2016).
[51] I. G. McCarthy, J. Schaye, S. Bird, and A. M. C. Le Brun, Mon. Not. R. Astron. Soc. 465, 2936 (2017).

[52] S. Genel, M. Vogelsberger, V. Springel, D. Sijacki, D. Nelson, G. Snyder, V. Rodriguez-Gomez, P. Torrey, and L. Hernquist, Mon. Not. R. Astron. Soc. **445**, 175 (2014).

[53] S. Foreman, W. Coulton, F. Villaescusa-Navarro, and A. Barreira, arXiv:1910.03597.

[54] M. P. van Daalen, I. G. McCarthy, and J. Schaye, Mon. Not. R. Astron. Soc. **491**, 2424 (2020).

[55] M. M. Ivanov, A. A. Kaurov, and S. Sibiryakov, J. Cosmol. Astropart. Phys. 03 (2019) 009.

[56] P. Valageas, Astron. Astrophys. **382**, 412 (2002).

[57] P. Valageas, Astron. Astrophys. **382**, 477 (2002).

[58] A. Caputo, H. Liu, S. Mishra-Sharma, and J. T. Ruderman (2020), https://github.com/smsharma/dark-photons-perturbations/blob/apr-2020/notebooks/09_plasma mass plot .ipynb.

[59] J. C. Mather, D. Fixsen, R. Shafer, C. Mosier, and D. Wilkinson, Astrophys. J. **512**, 511 (1999).

[60] See Supplemental Material at http://link.aps.org/supplemental/10.1103/PhysRevLett.125.221303 for additional details of the data analysis performed and a discussion of systematic effects, including citations to Refs. [22,23,33,34,48–52,55,56,61–78].

[61] G. D. Becker, J. S. Bolton, M. G. Haehnelt, and W. L. W. Sargent, Mon. Not. R. Astron. Soc. **410**, 1096 (2011).

[62] D. J. Fixsen, C. L. Bennett, and J. C. Mather, Astrophys. J. **526**, 207 (1998).

[63] F. Bernardeau and P. Reimberg, Phys. Rev. D **94**, 063520 (2016).

[64] C. Uhlemann, S. Codis, C. Pichon, F. Bernardeau, and P. Reimberg, Mon. Not. R. Astron. Soc. **460**, 1529 (2016).

[65] J. Betancort-Rijo and M. Lopez-Corredoira, Astrophys. J. **566**, 623 (2002).

[66] T. Y. Lam and R. K. Sheth, Mon. Not. R. Astron. Soc. **386**, 407 (2008).

[67] E. Adermann, P. J. Elahi, G. F. Lewis, and C. Power, Mon. Not. R. Astron. Soc. **479**, 4861 (2018).

[68] A. Dekel and O. Lahav, Astrophys. J. **520**, 24 (1999).

[69] L. Hurtado-Gil, V. J. Martínez, P. Arnalte-Mur, M. J. Pons-Bordería, C. Pareja-Flores, and S. Paredes, Astron. Astrophys. **601**, A40 (2017).

[70] A. Mead, C. Heymans, L. Lombriser, J. Peacock, O. Steele, and H. Winther, Mon. Not. R. Astron. Soc. **459**, 1468 (2016).

[71] Ya. B. Zeldovich, J. Einasto, and S. F. Shandarin, Nature (London) **300**, 407 (1982).

[72] A. Pisani et al., arXiv:1903.05161.

[73] J. Einasto, I. Suhhonenko, G. Hütsi, E. Saar, M. Einasto, L. J. Liivamägi, V. Müller, A. A. Starobinsky, E. Tago, and E. Tempel, Astron. Astrophys. **534**, A128 (2011).

[74] E. Jennings, Y. Li, and W. Hu, Mon. Not. R. Astron. Soc. **434**, 2167 (2013).

[75] K. C. Chan, N. Hamaus, and V. Desjacques, Phys. Rev. D **90**, 103521 (2014).

[76] M. Plionis and S. Basilakos, Mon. Not. R. Astron. Soc. **330**, 399 (2002).

[77] N. Schuster, N. Hamaus, A. Pisani, C. Carbone, C. D. Kreisch, G. Pollina, and J. Weller, J. Cosmol. Astropart. Phys. 12 (2019) 055.

[78] S. J. Witte, S. Rosauro-Alcaraz, S. D. McDermott, and V. Poulin, J. High Energy Phys. 06 (2020) 132.

[79] A. Kogut et al., J. Cosmol. Astropart. Phys. 07 (2011) 025.

[80] L. Davis, Jr., A. S. Goldhaber, and M. M. Nieto, Phys. Rev. Lett. **35**, 1402 (1975).

[81] P. Pani, V. Cardoso, L. Gualtieri, E. Berti, and A. Ishibashi, Phys. Rev. Lett. **109**, 131102 (2012).

[82] M. Baryakhtar, R. Lasenby, and M. Teo, Phys. Rev. D **96**, 035019 (2017).

[83] V. Cardoso, O. J. C. Dias, G. S. Hartnett, M. Middleton, P. Pani, and J. E. Santos, J. Cosmol. Astropart. Phys. 03 (2018) 043.

[84] M. Ahlers, J. Jaeckel, J. Redondo, and A. Ringwald, Phys. Rev. D **78**, 075005 (2008).

[85] M. Battaglieri et al., in U.S. Cosmic Visions: New Ideas in Dark Matter College Park, MD, USA, 2017 (2017), https://www.osti.gov/biblio/1409838.

[86] A. Caputo, H. Liu, S. Mishra-Sharma, and J. T. Ruderman (2020), https://github.com/smsharma/dark-photons-perturbations/blob/apr-2020/notebooks/02_firas_dp_limits .ipynb.

[87] A. Caputo, H. Liu, S. Mishra-Sharma, and J. T. Ruderman (2020), https://github.com/smsharma/dark-photons-perturbations/blob/apr-2020/notebooks/05_dp_dm_He_limits.ipynb.

[88] J. S. Bolton, G. D. Becker, M. G. Haehnelt, and M. Viel, Mon. Not. R. Astron. Soc. **438**, 2499 (2014).

[89] E. Boera, M. T. Murphy, G. D. Becker, and J. S. Bolton, Mon. Not. R. Astron. Soc. **441**, 1916 (2014).

[90] A. Rorai, R. F. Carswell, M. G. Haehnelt, G. D. Becker, J. S. Bolton, and M. T. Murphy, Mon. Not. R. Astron. Soc. **474**, 2871 (2018).

[91] H. Hiss, M. Walther, J. F. Hennawi, J. Oñorbe, J. M. O'Meara, A. Rorai, and Z. Lukić, Astrophys. J. **865**, 42 (2018).

[92] M. Walther, J. Oñorbe, J. F. Hennawi, and Z. Lukić, Astrophys. J. **872**, 13 (2019).

[93] A. Mirizzi, J. Redondo, and G. Sigl, J. Cosmol. Astropart. Phys. 08 (2009) 001.

[94] K. Choi, H. Seong, and S. Yun, arXiv:1911.00532.

[95] M. Pospelov, J. Pradler, J. T. Ruderman, and A. Urbano, Phys. Rev. Lett. **121**, 031103 (2018).

[96] T. Moroi, K. Nakayama, and Y. Tang, Phys. Lett. B **783**, 301 (2018).

[97] K. N. Abazajian et al. (CMB-S4 Collaboration), arXiv:1610.02743.

[98] P. Ade et al. (Simons Observatory Collaboration), J. Cosmol. Astropart. Phys. 02 (2019) 056.

[99] A. Caputo, H. Liu, S. Mishra-Sharma, and J. T. Ruderman (2020), https://doi.org/10.5281/zenodo.4081407.

[100] A. M. Price-Whelan et al., Astron. J. **156**, 123 (2018).

[101] T. P. Robitaille et al. (Astropy Collaboration), Astron. Astrophys. **558**, A33 (2013).

[102] A. Lewis, A. Challinor, and A. Lasenby, Astrophys. J. **538**, 473 (2000).

[103] A. Lewis and S. Bridle, Phys. Rev. D **66**, 103511 (2002).

[104] F. Perez and B. E. Granger, Comput. Sci. Eng. **9**, 21 (2007).

[105] T. Kluyver et al., in Positioning and Power in Academic Publishing: Players, Agents and Agendas (IOS Press, 2016), pp. 87–90, http://dx.doi.org/10.3233/978-1-61499-649-1-87.

[106] J. D. Hunter, Comput. Sci. Eng. **9**, 90 (2007).
[107] N. Hand, Y. Feng, F. Beutler, Y. Li, C. Modi, U. Seljak, and Z. Slepian, Astron. J. **156**, 160 (2018).
[108] S. van der Walt, S. C. Colbert, and G. Varoquaux, Comput. Sci. Eng. **13**, 22 (2011).
[109] M. Waskom *et al.*, mwaskom/seaborn:v0.8.1 (2017).
[110] W. McKinney, in *Proceedings of the 9th Python in Science Conference*, edited by S. van der Walt and J. Millman (2010), pp. 51—56, http://dx.doiorg/10.25080/Majora-92bf1922-00a.
[111] P. Virtanen *et al.*, Nat. Methods **17**, 261 (2020).
[112] C. O. da Costa-Luis, J. Open Source Softw. **4**, 1277 (2019).